AD-A039 212 LOCKHEED MISSILES AND SPACE CO INC PALO ALTO CALIF PA--ETC F/G 20/5
EXPERIMENTAL STUDY OF THE INITIATION MECHANISM OF LASER-SUPPORT--ETC(U)
FEB 77 T E SHARP
F44620-75-C-0041

UNCLASSIFIED LMSC-D556808 AFOSR-TR-77-0616 NL

| OF |
AD A039212

END

DATE FILMED
5-77

Interim Report

for the

Period

1 January 1976 - 15 February 1977

for

Air Force Office of Scientific Research

Contract Number F44620-75-C-0041

EXPERIMENTAL STUDY OF THE INITIATION MECHANISM OF LASER SUPPORTED ABSORPTION WAVES

T. E. Sharp
Nuclear Sciences Laboratory
Physical Sciences
Lockheed Palo Alto Research Laboratory
3251 Hanover Street
Palo Alto, California 94304

February 1977

LOCKHEED PALO ALTO RESEARCH LABORATORY
LOCKHEED MISSILES & SPACE COMPANY, INC

Section 1
INTRODUCTION

This report describes the work completed through the second year of the contract for an experimental investigation into the basic mechanism for formation of prompt laser supported absorption waves created when laser pulses of high power density are directed onto target surfaces. The objective of the research is to provide a detailed understanding of the laser-surface interaction, under conditions when bulk vaporization does not occur, by examination of the properties of the ejected electrons.

In Section 2 a discussion of the technical background and current state of knowledge is given. Section 3 is devoted to the experimental program with a description of the results to date. A summary of the status of the project is given in Section 4.

Section 2
TECHNICAL BACKGROUND

This section contains a short summary describing the prompt initiation of laser-supported absorption waves (LSAW), the initiation mechanisms which have been proposed, and the proposed experimental tests to distinguish among these mechanisms. Next there is a discussion of a preliminary correlation of previous studies of electron emission from metal surfaces under intense laser radiation. Finally, a new model for initiation of laser-supported detonation waves is described.

Mechanisms for Prompt Initiation of LSAW

The phenomenon of prompt initiation of laser-supported detonation waves has now been observed by many experimenters. Typical are the experiments of C. T. Walters* who irradiated rolled Al surfaces in air with submicrosecond bursts of 10.6 μm photons from a CO_2 TEA laser. At irradiances greater than about $10^7 watt/cm^2$, he observed formation of a laser-supported detonation wave within 20 ns after the laser pulse reached peak power. The luminous wave moved through the air, away from the surface, absorbing the laser radiation and blocking delivery of power to the target. The mechanism responsible for prompt initiation of these waves has not yet been determined.

The currently viable mechanisms which might account for rapid pro-

---

*References are located at the end of this section.

duction of ionization at localized sites, from which an absorption wave could be quickly initiated, are listed below:

1) Localized vaporization of inclusions which may have higher absorptivity than the surrounding metal surface and poor thermal contact with the bulk of the metal leading to a plasma "microjet" of the inclusion material.
2) Thermionic emission from "hot spots" associated with surface imperfections.
3) Localized high-field electron emission from protrusions on the surface.
4) Multiphoton emission of electrons from the metal surface.

Experimental tests which can be used to distinguish among these mechanisms are listed in Table 2-1 together with the predicted result for each mechanism.

Electron Emission from Metals under Intense Laser Irradiation*

Electron emission from metal surfaces under intense laser irradiation has been observed, measured and reported by many investigators, notably Farkas et al, Knecht, Logothetis and Hartman, and Ahmad and Walsh. Initial assessment of the measurements of these investigators reveals apparently conflicting results and unexplained trends in the data. It now appears, however, that it may be possible to reconcile all these results

*H. Musal, Private communication.

into an overall phenomenological picture. This approach will be briefly outlined here.

Figure 2-1 shows, in a semi-quantitative manner, how the electron emission current from a laser-irradiated metal surface behaves as the intensity of the radiation is increased. The emission current density J is plotted versus the laser irradiance G (both on normalized logarithmic scales). The dominant feature of this schematic graph is the transition threshold at which the emission current increases markedly. This transition threshold irradiance has been arbitrarily located at unity on the normalized intensity scale.

At irradiances below the transition, the electron emission current obeys a true "multi-photon" photoelectric emission law; the emission current density increases with irradiance according to the relationship $J \sim G^n$, where n = integer value of $[1 + (\Phi/h\nu)]$, Φ is the work function of the metal surface, and $h\nu$ is the photon energy of the laser radiation. In this region the plot is a straight line with slope n. Several lines are drawn to show the effect of increasing work function within the constraint of constant n. In this regime the emission current is sensitive to the polarization of the laser radiation, and the emitted electrons appear to have medium to high energies (up to the order of 10 electron-volts).

At the transition intensity the electron emission increases with a slope of order ~ 15, which is to be compared to a typical slope of 2 or 3 (for ruby lasers) at the lower intensities. The current is observed to

TABLE 2-1

Experimental Tests and Predicted Results for Various Mechanisms for Initiation of Laser Supported Absorption Waves

EXPERIMENTAL VARIABLE	PREDICTED RESULT MECHANISM			
	THERMIONIC EMISSION	VAPORIZATION OF IMPURITIES	FIELD EMISSION	MULTI-PHOTON EMISSION
ELECTRON ENERGY (MEASURED)	LOW	MEDIUM	HIGH	MEDIUM
TIME OF ELECTRON EMISSION (MEASURED)	DELAYED	DELAYED	PROMPT	PROMPT
SHORT LASER PULSE	NO EMISSION	NO EMISSION	EMISSION	EMISSION
POLARIZATION OF LASER BEAM, CORRECTED FOR ABSORPTION	NO EFFECT	NO EFFECT	MAXIMUM AT $\perp$ TO SURFACE	?
ANGLE OF INCIDENCE AT FIXED POLARIZATION	COSINE FUNCTION	COSINE FUNCTION	SINE FUNCTION	?
SURFACE CLEANLINESS	MINOR	CRUCIAL	MINOR	MINOR
SURFACE ROUGHNESS	MINOR	MINOR	CRUCIAL	MINOR
WAVELENGTH, CORRECTED FOR TOTAL ABSORPTION	MINOR	MINOR	CRUCIAL	?

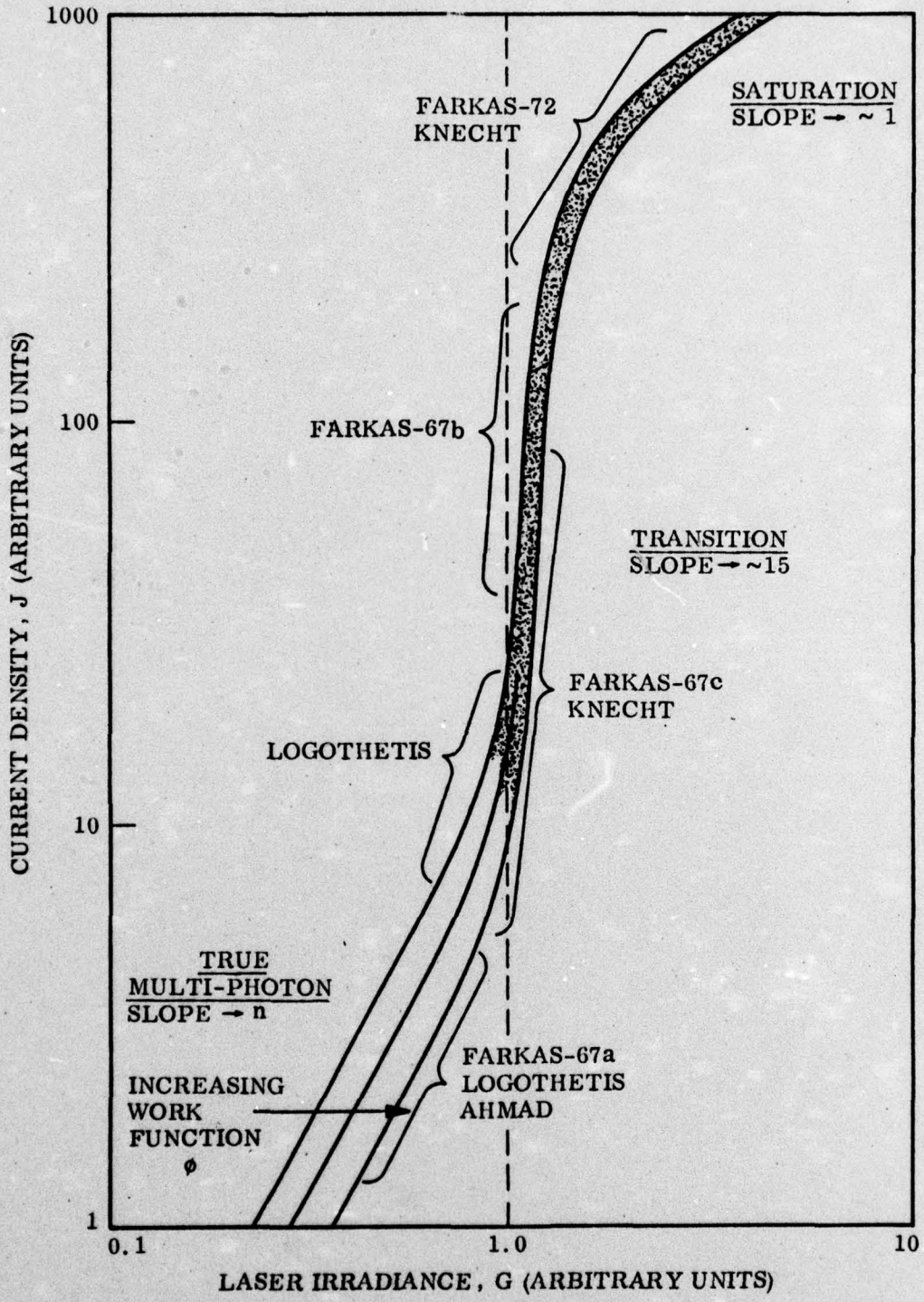

Fig. 2-1. Electron Emission from Metals under Intense Laser Radiation. The results of various investigators are correlated and located in the appropriate emission regimes: "true" multi-photon, transition, and saturation. For details, see text.

increase by many orders of magnitude. In this transition region the data display some sensitivity to the work function, but no data have been reported on the effects of polarization of the laser beam or on the energies of the emitted electrons.

At much higher irradiances the current density appears to display a saturation effect with the slope of the curve approaching unity.

With the above qualitative picture in mind, the experimental observations cited earlier can be put into context. This is shown in the figure by assignment of each observation to its appropriate regime. Thus, the data of Farkas - 67a on sensitivity of the electron emission to polarization of the laser radiation and the data of Logothetis and Hartman and of Ahmad and Walsh on the slope of the emission current curve, all fall in the true multi-photon emission regime and are consistent with each other. Some of the data obtained by Farkas -67c, by Knecht, and by Logothetis and Hartman span the intensity range between the true multi-photon emission regime and the transition regime. The data of Farkas -67b falls totally within the highly non linear transition regime. Finally, the saturation regime is appropriate to the data obtained by Farkas -72 and by Knecht. Most of the results cited above were obtained by using ruby laser although a very limited set of results were obtained with Nd:glass lasers and frequency-doubled ruby laser radiation. For ruby laser radiation, the incident threshold irradiance for the abrupt transition appears to be approximately 1 to 3 x 10^6 watt/cm^2.

It should be pointed out that this consolidation of available

experimental data on electron emission from laser-irradiated metal surfaces into an overall phenomenological picture is preliminary and somewhat speculative, and therefore requires further work for verification. In particular, the location of the transition threshold at other laser wavelengths is crucial to the development of wavelength scaling relationships. Also, a wider selection of metals of engineering importance should be studied. Finally, the physical mechanisms responsible for the transition and saturation behavior remain to be identified and analytically quantified.

Model for Initiation of Laser-Supported Detonation Waves

A model for the initiation of laser-supported detonation waves (LSDW) and its correlation with experimental data has been developed by Musal (H. Musal, ARPA Pulsed Laser Effects Workshop, La Jolla, California, 22-24 June 1976). By plotting the characteristics of all laser pulses which were reported to produce LSDW, he discovered two requirements for the production of these waves -

1) a minimum irradiation (power density) threshold, and
2) a minimum fluence (energy density) threshold. Both thresholds must be exceeded to produce LSDW. Neither the delivery of a very short, high power pulse nor the delivery of a large amount of energy in a long, low power pulse is sufficient to initiate a detonation wave.

The irradiation criterion requires that the power density of the laser pulse must exceed both of two values, one related to the properties

of the target and the other based on the properties of air. The irradiation threshold for metallic targets is 2.5×10^5 watt/cm^2 absorbed by the material. This is presumably the minimum irradiance required to eject enough energetic electrons from the target to seed an ionization cascade in the air close to the target. The irradiation threshold for subsequent growth of a fast, non-equilibrium ionization cascade in air is $(1 \times 10^6 \text{ watt/cm}^2)(10.6\ \mu\text{m}/\lambda)^2$, where λ is the wavelength of the laser.

The fluence criterion requires that the energy density of the laser pulse be sufficient for full development of the air plasma from a low electron density to the high electron density of a nearly fully ionized plasma. The fluence threshold is $(1 \text{ J/cm}^2)(10.6\ \mu\text{m}/\lambda)^2(1 \text{ atm}/P)$ where P is the ambient pressure.

Musal's two-criterion model gives a good fit to the existing LSDW data. A plot of fluence versus irradiance in the laser pulse provides a useful framework for correlating the existing experiments, and it has considerable predictive value. This is a significant achievement. It should be noted, however, that in its present form the model is fitted to observed gross data and does not deal in quantitative detail with the underlying physical processes. In particular, the mechanism of electron emission from the target is unspecified as is the mechanism by which the electrons acquire sufficient energy to initiate ionization. Additional experimental and theoretical work should refine the model.

An especially interesting aspect of the model which is amenable to testing by the experiments in this program is the wavelength scaling of the irradiation threshold. With CO_2 laser radiation at 10.6 μm, the material-dependent value (2.5×10^5 watt/cm^2 absorbed) and the intrinsic absorptivity of aluminum ($\alpha = 0.03$) lead to a threshold of 8×10^6 watt/cm^2 incident irradiance, to be compared with the air-dependent threshold of 1×10^6 watt/cm^2 incident irradiance

With the Nd:glass laser at 1.06 μm, the material-dependent threshold based on the absorptivity of aluminum at this wavelength ($\alpha = 0.1$) becomes 2.5×10^6 watt/cm^2, to be compared with the air-dependent threshold of 1×10^8 watt/cm^2. Thus, for aluminum subjected to pulses from the CO_2 laser, the irradiance threshold governing LSDW initiation should be material-dependent; but for pulses from the Nd:glass laser, the governing threshold should be dependent on the power density requirement for creating a fast cascade in the air.

Additional data which are to be provided by these experiments are the flux density and energy distribution of the electrons ejected from the target at or above the irradiance threshold. Coupling of this information to a theory of the breakdown of air by cascade ionization should lead to a satisfactory understanding of the physics of LSDW initiation.

REFERENCES

1. S. R. Ahmad and D. Walsh, "Photoelectric Emission from Metal Surfaces", J. Phys. D: Appl. Phys. 5, 1157-1159 (1972).
2. Gy. Farkas, Zs. Naray, and P. Varga, "Dependence of Non-Classical Electron Emission from Metals on the Direction of Polarization of Laser Beams", Phys. Lett. 24A, 134-135 (1967). Farkas -67a.
3. Gy. Farkas, I. Kertesz, Zs. Naray, and P. Varga, "On the Intensity Dependence of the Non-Linear Electron Emission from Silver Induced by a High Power Laser Beam", Phys. Lett. 24A, 475-476 (1967). Farkas-67b.
4. Gy. Farkas, I. Kertesz, Zs. Naray, and P. Varga, "On the Laser-Induced Non-Linear Photoelectric Effect in Metals", Phys. Lett. 25A, 572-573 (1967). Farkas-67c.
5. Gy. Farkas, Z. Gy. Horvath, and I. Kertesz, "Influence of Optical Field Emission on the Non-Linear Photoelectric Effect Induced by Ultra-Short Laser Pulses", Phys. Lett. 39A, 231-232 (1972).
6. W. L. Knecht, "Initial Energies of Laser-Induced Electron Emission from W", App. Phys. Lett. 6, 99-100 (1965).
7. E. M. Logothetis and P. L. Hartman, "Three-Photon Photoelectric Effect in Gold", Phy. Rev. Lett., 18, 581-583 (1967).
8. C. T. Walters and R. H. Barnes, "An Investigation of Mechanisms of Initiation of Laser-Supported Absorption (LSA) Waves". Battelle Columbus Laboratories, Semiannual Reports (November 1973, June 1974, with R. E. Beverley, III, Semiannual Report (January 1975) and Final Report (September 1975).

Section 3
EXPERIMENTAL PROGRAM

We plan to characterize the initiation mechanism for laser supported absorption waves by irradiating the target in vacuum and making measurements on the emitted electrons. The measurements include determination, as a function of laser power density and wavelength, of 1) the yield of electrons, 2) the energy spectrum, 3) the dependence on polarization, 4) the dependence on angle of incidence, and 5) the dependence on time during the pulse. As controls, we propose to make the same measurements on surfaces deliberately prepared 1) to contain a larger number of field emission points, 2) to contain a large concentration of absorptive inclusions, or 3) to be relatively pure and flat.

The target chamber and vacuum system were designed and built in the first-year phase of the contract. Their characteristics were described in the First Interim Report.

This section describes the experimental approach and the results obtained to date. First, the characteristics of the laser pulse are described, followed by a description of target materials. Then the performance of the electron energy spectrograph is discussed. Next the fast-response target is described. The results of the total-emission and the polarization-dependence experiments are presented. Finally, the implications of the data are considered.

Laser Pulse Characteristics

The data reported herein were obtained at 1.06 μm with single pulses selected from a Q-switched, mode-locked train from an Nd:glass laser and passed through two isolators located within four stages of amplification. The experiments were run concurrently with other studies which required higher irradiance. To do this, approximately 10% of the beam was split out with a pellicle located just upstream from the fifth amplifier, and a mirror was used to reflect this weaker beam into the target chamber built for this experiment. Neutral density filters located in front of the focusing lens for the target attenuated the laser beam by factors of about 10^{-5} to 10^{-3} to cover the desired range of irradiance (10^{6} to 10^{8} w/cm^2). The pulse length of the laser was measured as 125 ± 25 ps by a streak camera, where the limits include the pulse-to-pulse variations. The area of the target spot was taken as the area of the circular white spot (about 1.5 mm in diameter) produced on blackened polaroid print by an unattenuated, focused laser pulse. The average area was 1.84 ± 0.02 mm^2.

The energy in each pulse was obtained from a calorimetric monitor of the main laser beam which in turn was calibrated against a calorimeter placed in the beam split-off for the experiments reported herein. The energy per pulse for these experiments ranged up to 0.2 J before attenuation.

The laser beam entering the target chamber was elliptically polar-

ized with the major axis at about 4:30 o'clock (looking into the target).

Target Materials

The targets which were studied are discussed below.

A high purity (> 99.9%) aluminum sample was chemically etched and cleaned in distilled water to provide a flat metal surface free of impurities.

A cast aluminum sample provides a metal surface containing a relatively large concentration of absorptive inclusions.

Two samples of commercial rolled aluminum plates were used in "as received" condition after washing with detergent, distilled water, and alcohol to remove surface contamination. Aluminum 6061-T6 has the composition 0.25 percent Cu, 0.6 percent Si, 1.0 percent Mg, 0.25 percent Cr, balance Al; and aluminum 2024-T3 has the composition 4.5 percent Cu, 0.6 percent Mn, 1.5 percent Mg, balance Al. In addition, the surface of one sample of Al 6061-T6 was roughened with "Scotchbrite" abrasive pad to provide an abraded surface for study.

A type of target containing a large number of field emission points was purchased from SRI. It consists of a regular array of microscopic cones on 1 mil centers produced by vacuum evaporation of copper through a screen onto a molybdenum substrate. As deposition proceeded, the holes in the screen filled up, less vapor was transmitted, and a

regular square array of field emission points was produced. The cones were then overcoated with aluminum. (These samples were not available in time for the experiments reported herein but will be studied subsequently.)

Electron Energy Spectrograph

The electron energy spectrograph has been calibrated and performs at close to design parameters. The target holder for the laser shots incorporates an electron gun pinhole source to permit in situ energy calibration of the spectrograph. Initial shots with the laser have produced large, bright spots requiring some modification of the spectrograph. These facts are discussed below. The design construction and calibration of the parallel plate electrostatic spectrograph for measurement of the energy spectrum of the emitted electrons is discussed in detail in the First Interim Report.

The energy calibration of the spectrograph is sensitive to the position of the electron source. This position is difficult to measure because of the odd angles involved and because the target is mounted from the base of the chamber and the spectrograph is mounted on the lid. Consequently, an empirical in situ alignment and calibration is provided by placing an electron filament behind a pinhole at one side of the target assembly, level with the target surface. The pinhole is visually located as close as possible to the best source location, and final adjustments to achieve the narrowest, brightest line at the output of the spectrograph

are accomplished in vacuum using the electron source. The energy calibration is then established by the bias on the filament. The laser focus is then brought into registration with the pinhole by use of the visible alignment beam passing along the laser axis. Finally, the target is displaced sideways to bring the target material into testing position.

When the analyzer was used with a laser shot, a large bright spot appeared on the screen at analyzing voltages corresponding to slightly less than the accelerating voltage from the target. This effect probably results from electrons produced at the solid plate at the rear of the analyzer by photons coming from the target. These spurious electrons mask the desired signal of electrons emitted from the target. To reduce this undesired current, the rear analyzer plate has been replaced by a high-transmission nickel grid which will maintain the electrical characteristics of the analyzer while permitting the photons to pass out of the analyzer.

Measurements of Total Electron Emission

The fast response target shown in Figure 3-1 was designed as an open-ended section of a 50 ohm transmission line in order to minimize stray reactances. The design formula for a 50 ohm line is given by

$$\tan(\theta_2/2) = \exp(5\sqrt{k}/6) \tan(\theta_1/2) \qquad (3\text{-}1)$$

where k is the dielectric constant of the line, θ_1 is the half-angle for the inner conical conductor and θ_2 is the half-angle for the outer conical conductor. For ease of construction θ_2 was chosen to be 90°; thus θ_1 becomes 47°. The target assembly was constructed to fit into half of

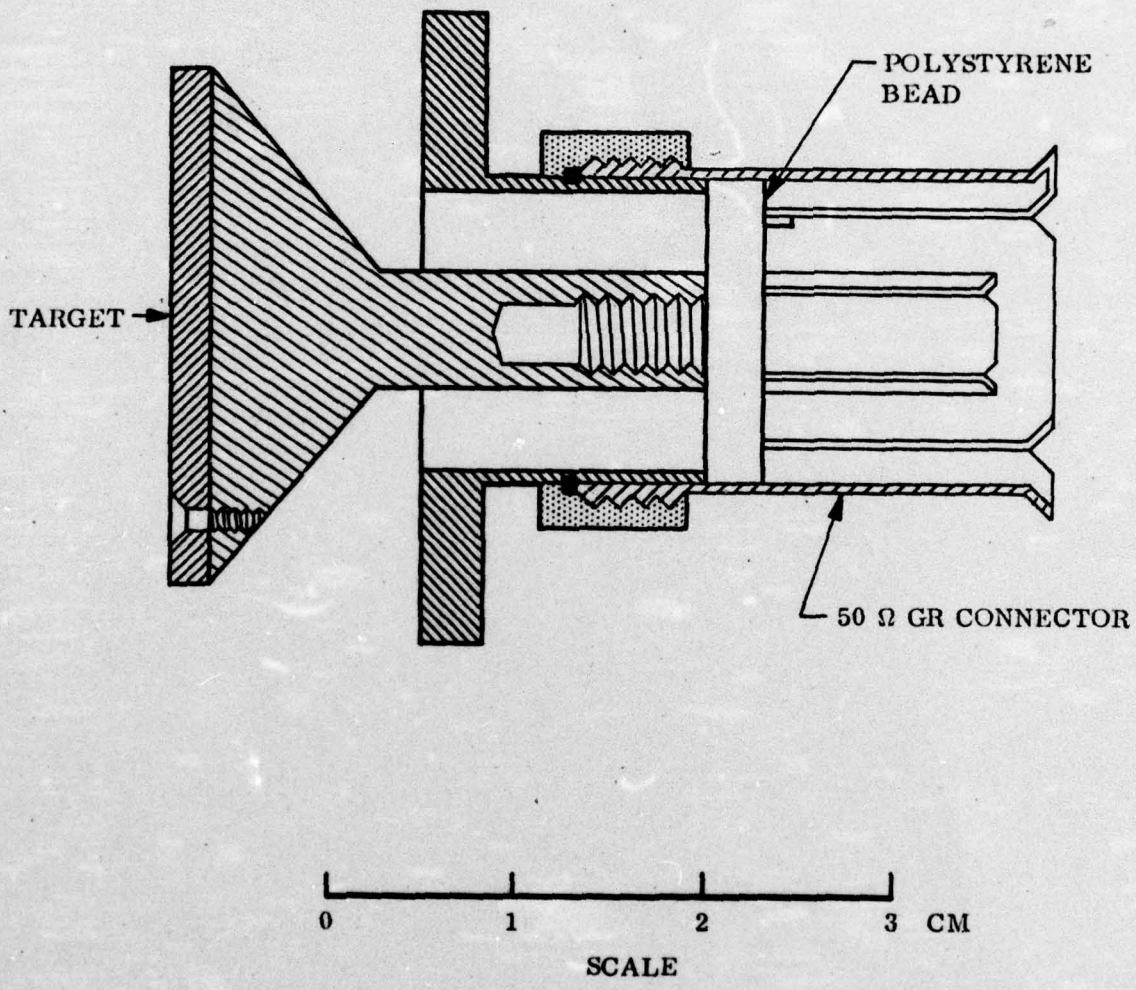

Fig. 3-1. Fast Response Target Assembly. Designed as an open-ended section of 50 ohm transmission line to minimize stray reactances.

a General Radio Type 874, 50 ohm connector. In use, an adapter connects the GR connector to 3 mm solid copper shielded 50 ohm line, to a 3 mm type connector through the wall of the vacuum chamber with similar cable to the Tektronix 7904 oscilloscope.

To register a voltage signal at the scope from the electrons ejected by a laser pulse on the target it was necessary to create a small drawout (of the order of 10V/cm) field at the target face. A planar electrode containing a hole of the same diameter as the target was located parallel to the target about 1 cm away. Biasing this electrode to a few hundred volts positive was sufficient to develop the electron signal. Repeated checks showed that the signal disappeared when the bias was removed. This behavior contrasts with the behavior observed by Walters at 10.6 μm with longer pulses (C. T. Walters, private communication) where large signals from photoemitted electrons were obtained without the use of a drawout field. It remains to be proved whether this difference in behavior has fundamental significance or is merely an experimental artifact.

The time-dependence of the electron current pulses were found to vary with increasing irradiance in the short laser pulse. As shown in Figure 3-2a, for relatively low irradiance, the electron pulse is a sharp spike. As the irradiance is increased, a tail with a longer time constant appears on the trailing edge of the pulse (Figure 3-2b). At the highest power densities studied the initial spike completely disappears, and both

20

a. 20 mv/div

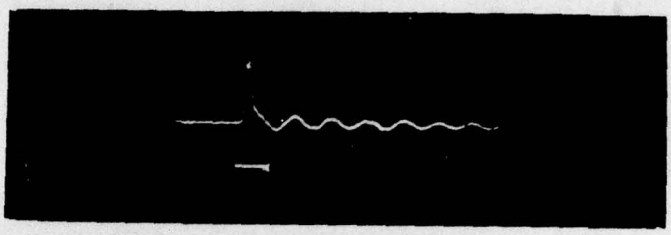

10 ns/div G_p = 30 Mw/cm^2

b. 50 mv/div

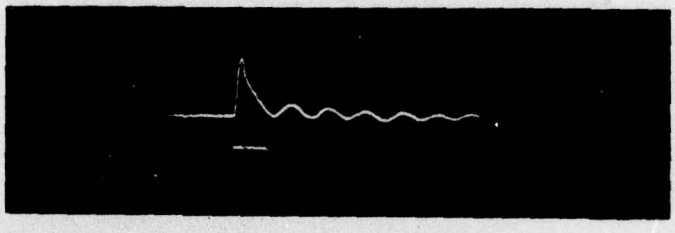

10 ns/div G_p = 160 Mw/cm^2

c. 100 mv/div

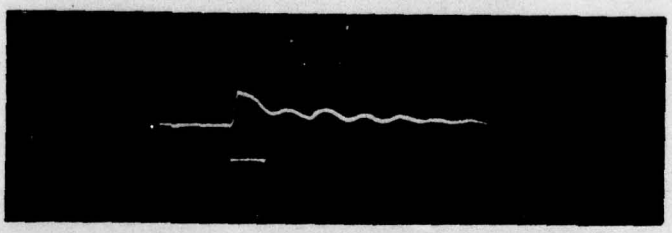

10 ns/div G_p = 290 Mw/cm^2

Fig. 3-2. Oscilloscope Traces of Total Electron Emission Versus Time for Three Different Incident Peak Laser Irradiances, G_p. Short horizontal line is one division.

a slower rise and long decay occur (Figure 3-2c). These results suggest the dominant electron-emitting process shifts from a prompt emission mechanism (for example, enhanced field emission) to a delayed emission mechanism (for example, thermionic emission) with increasing irradiance.

A rough calculation of maximum temperature rise at the target supports these results. Assuming that the laser energy is deposited within the electromagnetic skin depth of the target and that no energy is conducted or radiated away, one can calculate an upper limit to the temperature rise ΔT from

$$\Delta T = \alpha(\Delta E)/(\delta \rho c_p) \qquad (3\text{-}2)$$

where α is the absorptivity (0.1 for Al at 1.06 μm), ΔE is the incident energy in the laser beam, δ is the deposition depth (15 μm), ρ is the target density, and c_p is the specific heat capacity of the target ($\rho c_p = 1\ J/cm^3$). For a 100 ps pulse of 1×10^6 w/cm^2 irradiance, the calculated temperature rise is 7 K while for a similar pulse of 1×10^8 w/cm^2, the rise is 700 K - an overestimate because the target spot would melt.

These initial results warrant more detailed investigation.

Plots of the peak electron current density J_p emitted as a function of laser irradiance for normal incidence of the laser beam on several targets are shown in Figures 3-3 to 3-5. The value of J_p was

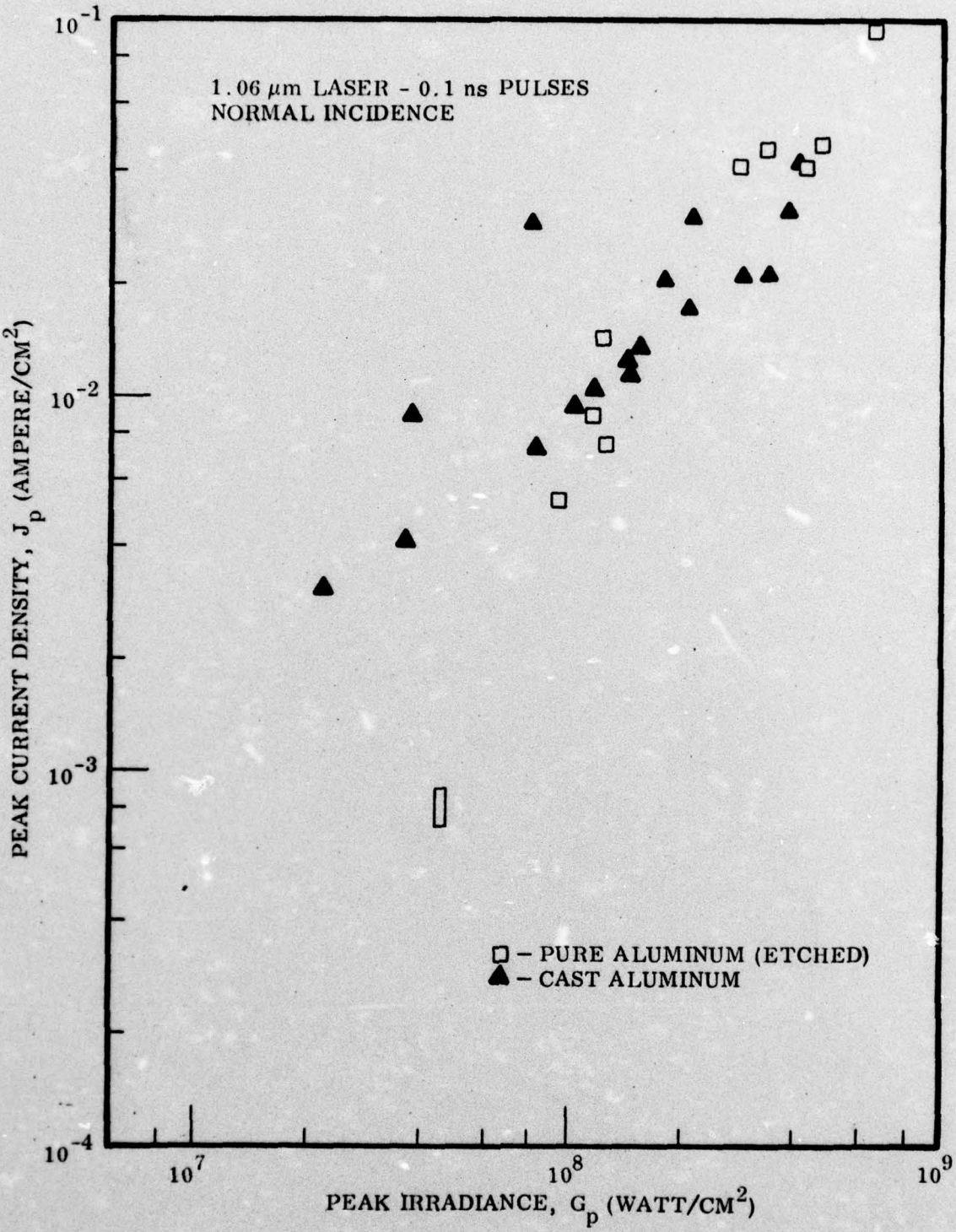

Fig. 3-3 Dependence of Electron Emission on Laser Irradiance Single pulses of 125 ± 25 ps duration were selected from a mode-locked, Q-switched train and focused to a 1.5 mm diameter spot. Target materials were high purity aluminum and cast aluminum.

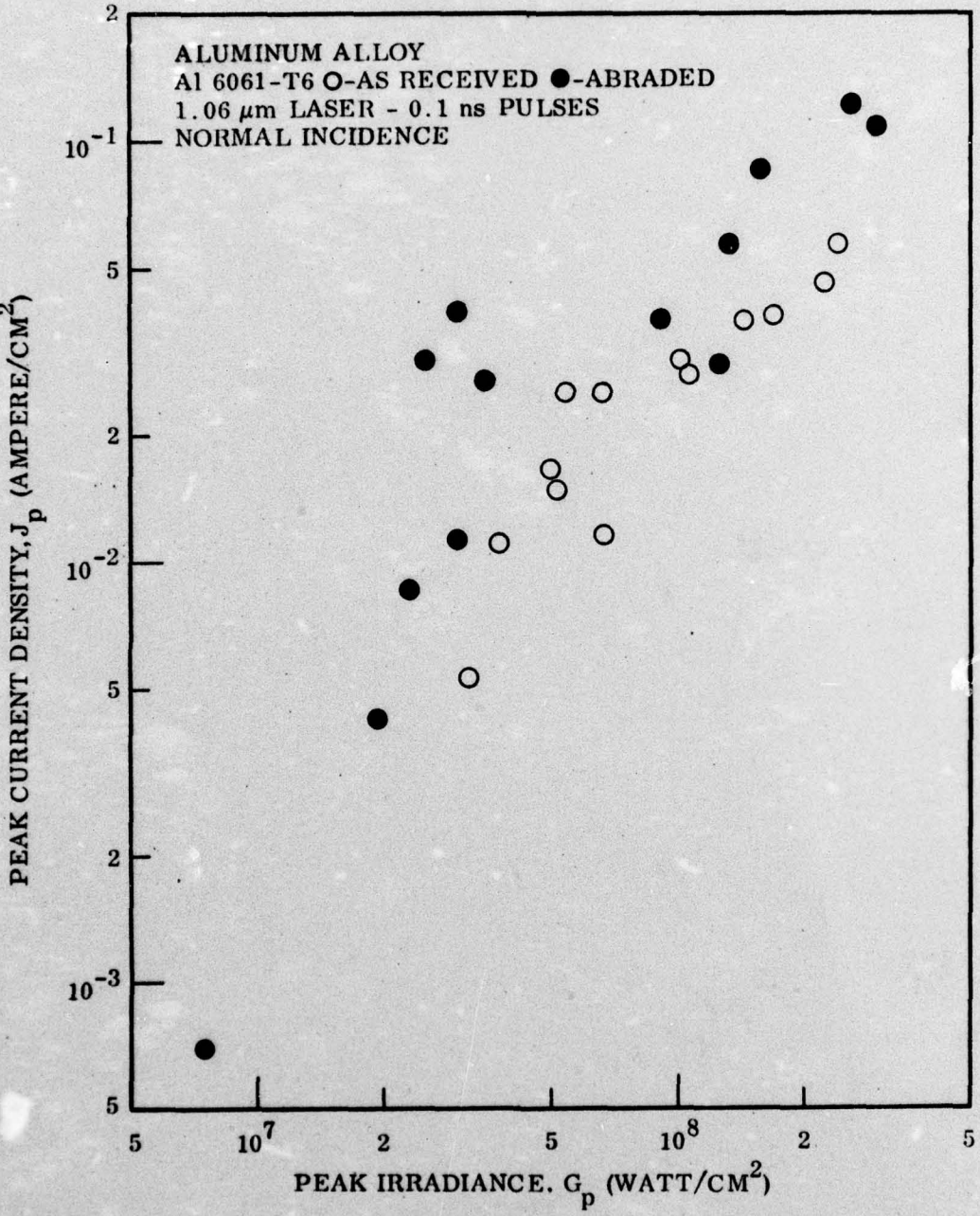

Fig. 3-4 Dependence of Electron Emission on Laser Irradiance. Target materials were "as received" and abraded targets of Aluminum 6061-T6 alloy.

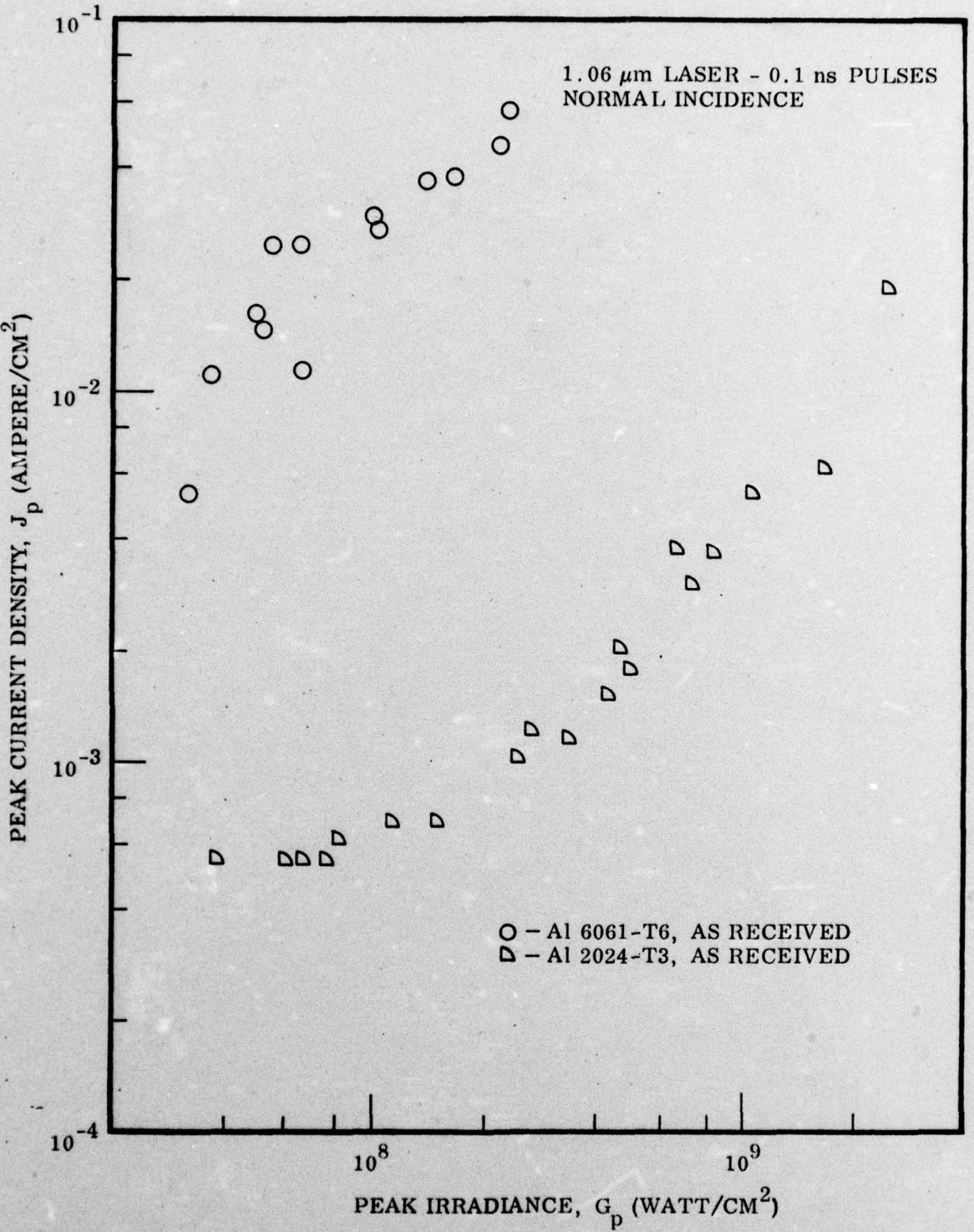

Fig. 3-5 Dependence of Electron Emission on Laser Irradiance. Target materials were "as received" aluminum 6061-T6 alloy and "as received" aluminum 2024-T3 Alloy

obtained by dividing the maximum voltage observed on the scope photograph by the 50 ohm scope termination and the area of the target spot. A new target spot was used for each laser pulse to avoid possible effects of annealing on a previous shot. A steady increase of electron emission with irradiance is observed, although there is appreciable scatter in the data. Note that the figures underemphasize the total emission of electrons at the higher irradiances because the long tail of the electron emission curve is not reflected in the plot of peak electron current density.

In Figure 3-3 the electron emission of cast aluminum, a surface containing a relatively large amount of absorptive inclusions is given together with that for high purity, chemically etched aluminum. Comparison of the data shows no significant difference in electron emission between the two materials, except possibly at the lowest irradiance studied. For these tenth-nanosecond pulses at 1.06 μm, the vaporization of absorptive inclusions does not appear to contribute significantly to the electron emission.

In Figure 3-4 is shown the electron emission from two different surface preparations of Al 6061-T6 alloy - "as received" and abraded. The abraded surface yields about twice the current density compared to the "as received" surface, indicating the enhancement effect of surface irregularities. Comparison with Figure 3-3 shows that the current density emitted by the "as received" Al 6061-T6 alloy is two to three times that of the high purity, flat aluminum. It is not clear whether this difference is due to the rolling and heat treatment in the production of

the alloy or to the metallic alloying materials.

In Figure 3-5 the electron emission from two different "as received" alloys is shown. The emission from Al 2024-T3 is nearly a factor of 50 smaller than that from Al 6061-T6. It is possible that the relatively large amount of copper in the 2024-T3 alloy reduces the density of electrons available for emission from the solid, but this point requires further investigation. At any rate, these results indicate that the probability of formation of an LSD wave from a target of Al 2024-T3 alloy should be considerably less than that from pure Al, cast Al, or 6061-T6 alloy.

Polarization Dependence of Electron Emission

For these experiments the fast response target described above was rotated 45° about a vertical axis, and the drawout electrode was shifted slightly to give an unobstructed view of the target from the lens. A polarizer was oriented along the major axis of the ellipse of polarization of the laser beam (45° ccw from the vertical) to assure linear polarization at the target. This was followed by a half-wave plate which was set with its principal axis at an angular displacement of 22.5° to either side of the direction of polarization. Setting the axis of the half-wave plate between the incident polarization and the vertical rotated the polarization direction to vertical, and the polarization vector of the beam striking the target fell along the target surface. Setting the axis of the half-wave

plate between the incident polarization and the horizontal rotated the polarization direction to horizontal, and the polarization vector of the beam striking the target had a large component perpendicular to the target surface.

The incident irradiance was computed from the measured energy, known pulse width, and the area of the elliptical white spot produced on a blackened polaroid print by an unattenuated, focused laser pulse ($3.90\ mm^2$). Because the half-wave plate had an effective diameter of only 0.5 inch (compared with an 0.875 inch diameter of the laser beam), the area of the smaller elliptical spot produced by the laser beam after passing through the collimator for the half-wave plate was used to calculate the electron current density ($0.99\ mm^2$).

The results of the polarization measurements on 6061-T6 Al alloy are shown in Figure 3-6. Because substantially more electrons are emitted when the polarization vector points out of the target than when it lies in the target plane, it is clear that the electron emission process is strongly influenced by the electric vector of the laser light as would be expected, for example, for an enhanced field emission mechanism but not for a purely thermal effect.

Electron emission from cast aluminum, however, is independent of the angle of polarization as shown in Figure 3-7. A mechanism which is independent of the direction of the electric vector of the laser light is

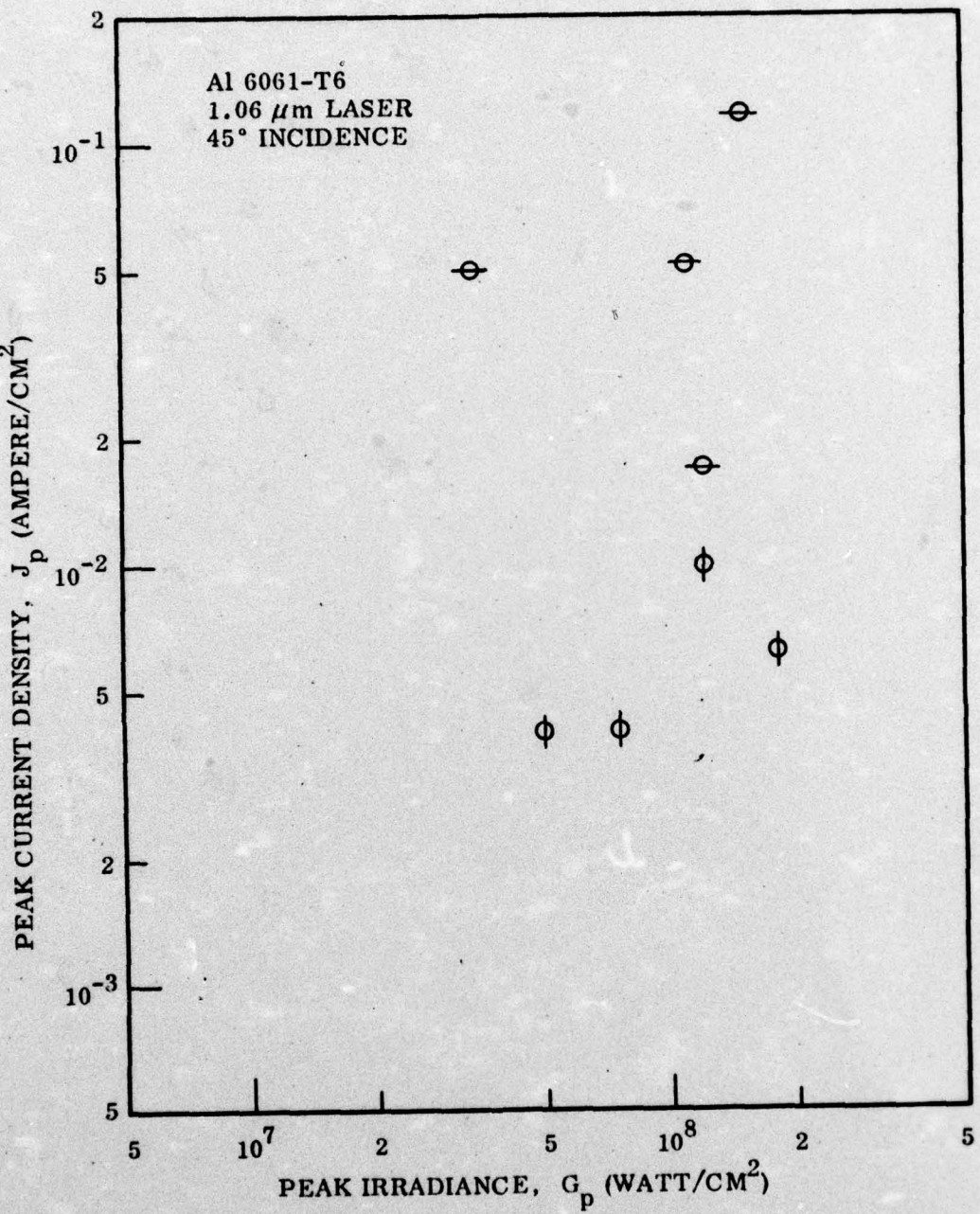

Fig. 3-6. Polarization Effect on Electron Emission. The direction of polarization of the laser radiation was parallel to the target plane for data points marked with vertical lines and perpendicular to the target plane for points with horizontal lines. The perpendicular orientation yielded greater electron emission.

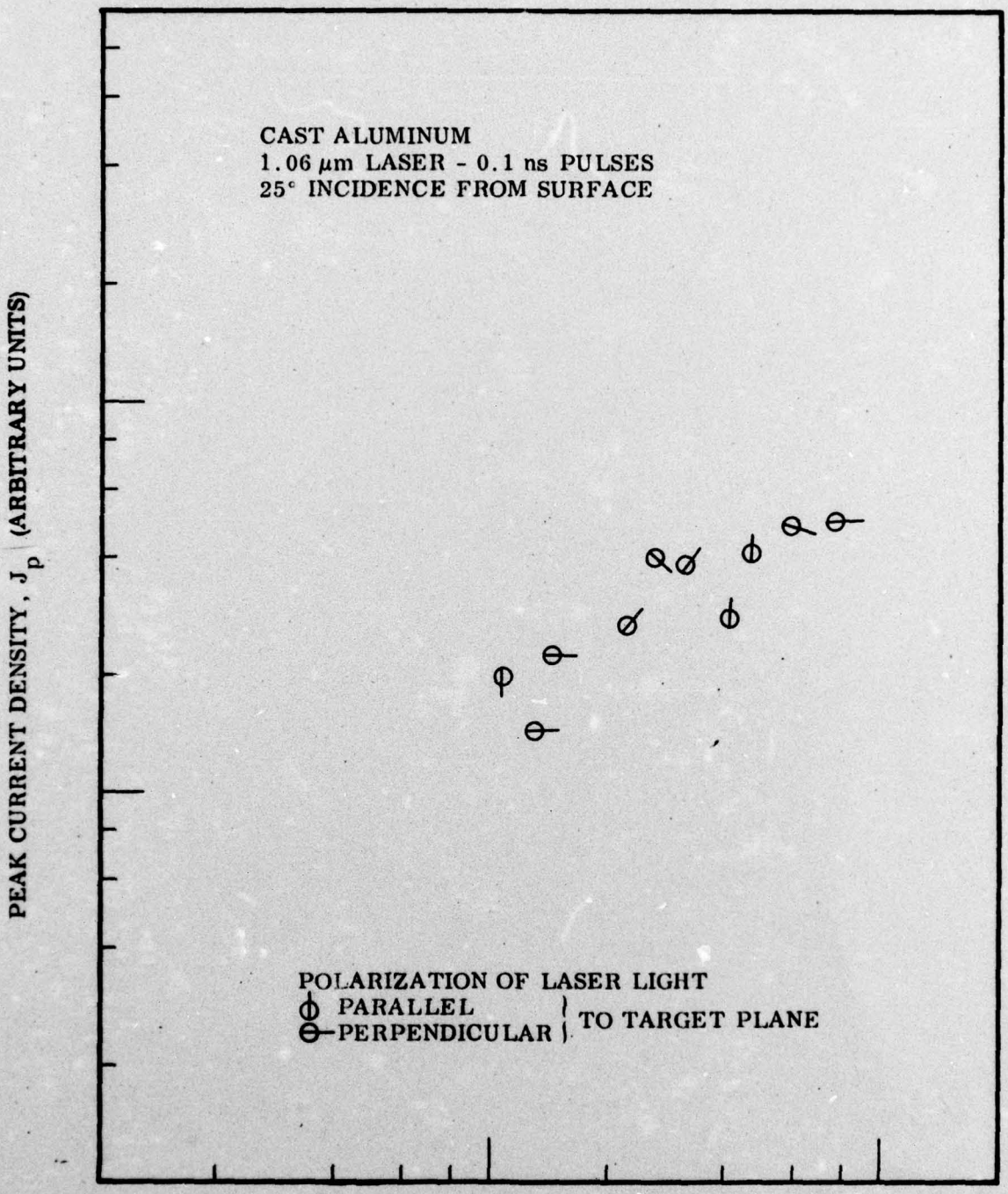

Fig. 3-7 Polarization Effect on Electron Emission. Target was cast aluminum. Emission of electrons is independent of direction of polarization of laser light.

pparently dominant for cast aluminum.

Discussion

The data obtained for 0.1 ns pulses of 1.06 μm laser radiation are compared with the anticipated results for various mechanisms for the initiation of LSA waves listed in Table 2-1. At the lowest irradiances, the electron emission appeared in a short pulse whose width corresponded to the minimum response time of the electronics. As the laser irradiance was increased, this sharp spike of electron emission developed a tail at longer times. At the highest irradiances, the electron emission pulse loses its "spike" appearance and exhibits both a slower rise and a longer decay. This behavior was observed for all the materials tested. The calculation of temperature rise (Equation 3-2) also supports the suggestion that the dominant electron-emitting process shifts from a prompt emission mechanism to a delayed emission mechanism. Alternatively, a space charge effect might also occur at the higher current densities, limiting the rate of rise of the electron emission pulse and extending its length. This could be tested by increasing the electron drawout field.

The polarization data for Al 6061-T6 show a strong dependence of electron emission on the polarization of the laser beam at both low and high intensities. This dependence is uncharacteristic of thermionic emission or of vaporization of inclusions but is expected for enhanced field emission and probably for multi-photon emission. The persistence of the polarization dependence to high irradiance levels is evidence against

a shift from one class of mechanism to another with increasing irradiance.

For cast aluminum the electron emission pulse shapes behave like those from Al 6061-T6, but electron emission is found to be independent of the polarization of the laser beam. These results are compatible with the multiphoton emission mechanism. However, the slope of the emission versus irradiance curve is not large enough to demonstrate a true multiphoton emission.

The slopes of the electron emission versus irradiance curves (Figures 3-3 to 3-5) are all close to unity. In the framework of phenomenological theory (Figure 2-1), the emission observed in these studies appears to be occurring in the "saturation" region. It would be highly desirable to extend the measurements to lower irradiance in order to locate the "transition" region and the "true multiphoton" region and to determine the characteristics of the emission mechanisms there. The electron current is expected to fall off rapidly at lower irradiances and would rapidly drop below the capability of our present electronics for the subnanosecond laser pulses. By using longer laser pulses, of the order of 10 nanoseconds, it becomes possible to use existing equipment (Avantek AD-9, risetime 0.7 ns) to amplify the electron signal by a factor of 50 without significant distortion.

Section 4
STATUS OF RESEARCH EFFORT

The research tasks designated for this contract and their current status are summarized.

Task a. "Design, develop, and test a high vacuum system capable of reaching a base pressure of 10^{-6} torr with windows for transmission of 1 μm and 10.6 μm laser light and containing a target positioner and provision for mounting an electron spectrograph." This has been accomplished.

Task b. "Design, develop, test, and calibrate an electrostatic parallel plate electron spectrograph with channel plate image intensifier for measuring and recording the yield and energy distribution of electrons ejected from the target by a laser pulse." This has been accomplished; however, experience with actual laser shots has demonstrated the need for use of a grid in the analyzer to eliminate spurious photoelectrons produced inside the spectrograph. The calibration of the yield of electrons ejected from the target will be completed after testing of this modification.

Task c. "Prepare or obtain special materials to be used as

targets to include a commercial rolled aluminum plate, a metal surface containing a large number of field emission points, a metal surface containing a large concentration of volatile impurities, and a metal surface which is relatively flat and free of impurities." This has been accomplished.

Task d. "Conduct laser pulse experiments using materials and apparatus developed during the first year of the program with both Nd:Glass laser and CO_2 laser, and varying laser power density, polarization of the laser radiation, and angle of incidence of the laser beam; and measure, in vacuum, the energy, current, and time characteristics of electrons emitted from the target as a function of laser beam properties for different materials selected to enhance or reduce optical field emission." Experiments using subnanosecond pulses from the Nd:Glass laser have been completed. These experiments demonstrated the desirability of using longer pulses from the Nd:Glass laser. Due to technical difficulties, the CO_2 laser experiments had to be delayed beyond this reporting period.

Task e. "Compare the observed electron characteristics measured for cases where laser supported absorption waves are produced in air with cases where no waves are produced." This is continuing.

Task f. "Perform data analysis and infer the adequacy or inadequacy of the theoretical model by comparison of experimental results with the theory." This is continuing.

Task g. "Conduct additional laser pulse experiments using the apparatus already developed under this program, with visible (frequency doubled Nd laser) light in addition to infrared laser light and varying laser irradiance, polarization of the laser radiation, and angle of incidence of the laser beam; and measure, in vacuum, the energy, current, and time characteristics of electrons emitted from the target as a function of laser beam properties for different materials, both bare and with simple coatings, selected to enhance or reduce optical field emission of electrons." This work is scheduled for the third phase of the contract. Sample targets of interest to the Air Force have been received from the AF Materials Laboratory, Wright-Patterson AFB.

No publications have resulted from the second year's effort. A verbal presentation on this project was given by T. E. Sharp at the ARPA Pulsed Laser Effects Workshop, La Jolla, California, 22-24 June 1976. No major deviations are contemplated in this program. The research is expected to be completed on schedule.

Unclassified

SECURITY CLASSIFICATION OF THIS PAGE (When Data Entered)

(18) (19)

REPORT DOCUMENTATION PAGE

READ INSTRUCTIONS BEFORE COMPLETING FORM

1. REPORT NUMBER: AFOSR - TR - 77 - 0616
2. GOVT ACCESSION NO.
3. RECIPIENT'S CATALOG NUMBER: (rept.)

(6) 4. TITLE (and Subtitle): Experimental Study of the Initiation Mechanism of Laser Supported Absorption Waves.

(9) 5. TYPE OF REPORT & PERIOD COVERED: INTERIM 1 Jan [illegible] 76 - 15 Feb [illegible] 77

6. PERFORMING ORG. REPORT NUMBER

(10) 7. AUTHOR(s): T. E. Sharp

(15) 8. CONTRACT OR GRANT NUMBER(s): F44620-75-C-0041 new

9. PERFORMING ORGANIZATION NAME AND ADDRESS
Lockheed Missiles & Space Company, Inc.
Palo Alto Research Laboratory
3251 Hanover Street
Palo Alto, California 94304

10. PROGRAM ELEMENT, PROJECT, TASK AREA & WORK UNIT NUMBERS
9767-04
61102F

11. CONTROLLING OFFICE NAME AND ADDRESS
Air Force Office of Scientific Research
Bldg. 410 Bolling AFB, Washington, D.C. 20332

(11) 12. REPORT DATE: 22 Feb [illegible] 77
13. NUMBER OF PAGES

14. MONITORING AGENCY NAME & ADDRESS (if different from Controlling Office)

(12) 36p.

15. SECURITY CLASS. (of this report): Unclassified

15a. DECLASSIFICATION/DOWNGRADING SCHEDULE

16. DISTRIBUTION STATEMENT (of this Report)

Distribution of this document is unlimited.

(16) 9767

(17) 04

17. DISTRIBUTION STATEMENT (of the abstract entered in Block 20, if different from Report)

(14) LMSC-D556808

18. SUPPLEMENTARY NOTES

19. KEY WORDS (Continue on reverse side if necessary and identify by block number)

Laser - Supported Absorption Waves
Laser - Supported Detonation Waves
Laser Interaction with Materials
Plasma Diagnostics

20. ABSTRACT (Continue on reverse side if necessary and identify by block number)

Mechanisms for prompt initiation of laser supported absorption waves are identified with their experimental consequences. A phenomenological theory of electron emission from metals under intense laser irradiation is discussed. A recent model for initiation of laser supported detonation waves which requires exceeding both irradiation and fluence thresholds is summarized.

Experiments with 0.1 ns pulses of 1.06 micrometers laser light with irradiance from

Over

DD FORM 1 JAN 73 1473 EDITION OF 1 NOV 65 IS OBSOLETE

Unclassified

SECURITY CLASSIFICATION OF THIS PAGE (When Data Entered)

210 118

20. (Continued) 59 cm
8 to 250 Mw/cm² on various aluminum targets in vacuum are described. Data are given for the time dependence and peak current density of electron emission as a function of laser irradiance and for the dependence of electron emission on laser polarization. The implications of the data for initiation mechanisms is discussed.